



HAL
open science

Nitrogen diffusion through cementite layers

Marc Nikolussi, Andreas Leineweber, Eric Jan Mittemeijer

► **To cite this version:**

Marc Nikolussi, Andreas Leineweber, Eric Jan Mittemeijer. Nitrogen diffusion through cementite layers. *Philosophical Magazine*, 2010, 90 (09), pp.1105-1122. 10.1080/14786430903292365. hal-00581014

HAL Id: hal-00581014

<https://hal.science/hal-00581014>

Submitted on 30 Mar 2011

HAL is a multi-disciplinary open access archive for the deposit and dissemination of scientific research documents, whether they are published or not. The documents may come from teaching and research institutions in France or abroad, or from public or private research centers.

L'archive ouverte pluridisciplinaire **HAL**, est destinée au dépôt et à la diffusion de documents scientifiques de niveau recherche, publiés ou non, émanant des établissements d'enseignement et de recherche français ou étrangers, des laboratoires publics ou privés.



Nitrogen diffusion through cementite layers

Journal:	<i>Philosophical Magazine & Philosophical Magazine Letters</i>
Manuscript ID:	TPHM-09-Jul-0301.R1
Journal Selection:	Philosophical Magazine
Date Submitted by the Author:	20-Aug-2009
Complete List of Authors:	Nikolussi, Marc; Max Planck Institute for Metals Research,, Department Mittemeijer Leineweber, Andreas; Max Planck Institute for Metals Research, Department Mittemeijer Mittemeijer, Eric Jan; Max Planck Institute for Metals Research, Prof. Dr Ir. E.J. Mittemeijer
Keywords:	carbides, diffusion, nitrides, thermodynamics
Keywords (user supplied):	cementite, nitrocarburising, activation energy



Nitrogen diffusion through cementite layers

Marc Nikolussi, Andreas Leineweber, Eric Jan Mittemeijer

Max Planck Institute for Metals Research, Heisenbergstrasse 3, D-70569 Stuttgart, Germany

Abstract – Massive cementite layers with a time-dependent thickness were grown on ferrite substrates by nitrocarburising in a dedicated $\text{NH}_3/\text{H}_2/\text{CO}/\text{N}_2$ containing gas atmosphere at 783 K, 823 K and 843 K. Nitrogen diffusion through the cementite layer into the ferrite substrate took place in conjunction with growth of the cementite layer; a significant, i.e. measurable solubility of nitrogen in cementite was not observed. The nitrogen concentration-depth profiles in the substrate, underneath the growing cementite layer, were quantitatively determined using a calibrated microhardness-measurement technique. The nitrogen concentration-depth profiles were simulated on the basis of a model using an implicit finite-difference method. The simulation yielded values for the diffusivity of nitrogen through cementite, including the activation energy.

Keywords: cementite; nitrogen diffusion; activation energy; nitrocarburising; nitriding

1. Introduction

The corrosion and wear resistances of iron-based workpieces as well as the fatigue endurance can be improved pronouncedly by thermochemical heat treatments such as nitriding and nitrocarburising which are of great technological importance [1, 2].

Gaseous nitriding and gaseous nitrocarburising are usually performed at temperatures between 773 K and 853 K. Thus, the process temperature is located below the binary/ternary eutectoid temperature of the Fe-N/Fe-N-C solid solution [3, 4]. The nitriding/nitrocarburising gas atmosphere provides nitrogen or nitrogen and carbon, which are taken up by the surface-region of the iron-based workpieces [5].

The incorporation of nitrogen or nitrogen and carbon results in (i) the formation of a compound layer (several 10 μm thick) and/or (ii) the formation of a diffusion zone (several 100 μm thick). The compound layer is responsible for a considerable enhancement of the corrosion and wear resistance. Depending on the treatment temperature, the pressure and the composition of the gas atmosphere, the compound layer can consist of different phases. Typically γ' -Fe₄N_{1-y} and ϵ -Fe₃(N,C)_{1+x} are constituents of the compound layer [6] but also cementite can occur in the compound layer [7, 8]. The diffusion zone is responsible for a considerable enhancement of the fatigue endurance [9]. Nitrogen or nitrogen and carbon are dissolved (at the treatment temperature) as solid solution in the octahedral interstices of the iron bcc-lattice.

It was shown recently that, under certain conditions, also pure, massive cementite layers can form on the ferrite substrate [8]. These cementite layers have been investigated in detail with respect to their homogeneous cementite-phase microstructure, with respect to conditions for occurrence of additional (carbo)nitride phases and the corresponding phase equilibria as well as with respect to selected mechanical properties [8, 10, 11, 12, 13, 14].

In the presence of cementite compound layers it turns out that the nitrogen (and carbon) diffusion into the substrate is strongly decelerated; cementite acts as a diffusion barrier for

1
2
3 nitrogen [15] and carbon [16]. Nonetheless, although nitrogen transport through cementite is
4
5 decelerated, it is shown in this paper that a certain time-dependent amount of nitrogen is
6
7 transported through the cementite into the ferrite substrate, leading to an increase of the
8
9 nitrogen content in (and the hardness of) the ferrite substrate. The solubility of nitrogen in the
10
11 ferrite is much higher than for carbon at the temperatures of interest (783 K – 843 K), e.g.
12
13 values of 0.29 at.-% for nitrogen vs. ≈ 0.012 at.-% for carbon at 823 K are found in Ref. [17].
14
15 Furthermore, most of the carbon incorporated in the solid is used to build up the cementite
16
17 layer, whereas nitrogen passes through the cementite layer to be dissolved in the ferrite.
18
19
20
21

22 The present work focuses on the diffusion of nitrogen through cementite. Hardness-
23
24 depth profile measurements in the ferrite substrate are used to determine the nitrogen
25
26 concentration-depth profiles. A model is proposed that enables the simulation of such nitrogen
27
28 concentration-depth profiles. On this basis, for the first time, information about the diffusivity
29
30 of nitrogen *through* cementite, including the corresponding activation energy of nitrogen
31
32 diffusion in cementite, is obtained.
33
34
35
36
37
38

39 2. Experimental

40 41 2.1 Specimen preparation and gaseous nitriding/nitrocarburising

42
43 Two differently produced types of specimens were investigated in this study: “Thick-plate”
44
45 specimens for *nitrocarburising* experiments were produced by cold-rolling a ferrite cast rod
46
47 (Alfa Aesar, 99.98 wt.-% Fe) on both sides to a thickness of 1 mm. From the resulting cold-
48
49 rolled sheet, rectangular pieces (20 mm \times 25 mm) were cut, ground, polished (final stage 1
50
51 μm diamond suspension) and cleaned ultrasonically in ethanol. “Thin-plate” specimens for
52
53 *nitriding* experiments were produced by cutting from a 10 cm \times 10 cm iron sheet (Alfa Aesar,
54
55 99.98 wt.-% Fe) of 0.1 mm thickness rectangular pieces of 20 mm \times 25 mm which were
56
57 ground, polished (final stage 1 μm diamond suspension) and cleaned ultrasonically in ethanol.
58
59
60
61 In order to remove the cold deformation both types of specimens were, prior to gaseous

1
2
3 nitriding/nitrocarburising, recrystallised at 973 K for 2 h under a reductive hydrogen flow of
4
5 200 ml min⁻¹, polished (final stage 1 µm diamond suspension) and cleaned ultrasonically in
6
7 ethanol.
8
9

10 The nitriding/nitrocarburising facility had to ensure the desired gas environment and the
11
12 desired temperature during treatment. Moreover, it was necessary to quench the specimens
13
14 after treatment in order to retain the microstructure as at the treatment temperature. Thus, the
15
16 nitriding/nitrocarburising facility was composed of a vertical quartz-tube furnace which was
17
18 at its end equipped with a water (flushed with N₂) container for quenching the specimens to
19
20 room temperature. Using a quartz fibre, which, to realise quenching, can mechanically be
21
22 destroyed after the nitriding/nitrocarburising treatment, the specimens prepared as described
23
24 above were positioned in the middle of the quartz-tube furnace where the process temperature
25
26 (controlled within ± 1 K) prevailed.
27
28
29
30

31
32 Two types of treatments were conducted in the present work: (i) *Nitrocarburising*
33
34 experiments to study nitrogen diffusion through growing cementite layers, and (ii) *nitriding*
35
36 experiments to prepare specimens of homogeneous nitrogen content and without compound
37
38 layer. For these experiments, ammonia (99.999 vol.-%) as nitrogen supply, carbon monoxide
39
40 (99.97 vol.-%) as carbon supply, hydrogen (99.999 vol.-%), and nitrogen (99.999 vol.-%), as
41
42 inert gas, were employed. Each gas flux was controlled by a separate mass-flow controller.
43
44 An overall linear flow rate of 13.5 mm s⁻¹ (calculated for the gas volume at room temperature)
45
46 through the quartz retort (diameter 28 mm) was maintained. Such a flow rate ensures that
47
48 ammonia dissociation, which would change the composition of the gas atmosphere, can be
49
50 neglected.
51
52
53
54

55 For gaseous *nitrocarburising* the gas atmosphere was composed of 13 vol.-% NH₃, 58
56
57 vol.-% H₂ (nitriding potential¹ $r_N = 0.3 \text{ atm}^{-1/2}$), 20 vol.-% CO and 9 vol.-% N₂ (as inert gas).
58
59

60
¹ The chemical potential of nitrogen in the gas atmosphere can be related with the nitriding potential [18]. In the present work no carburising potential can be adjusted: the carburising potential for a gas atmosphere composed

1
2
3 The experiments were performed at $T = 783$ K, 823 K and 843 K, for treatment times of 0.5 h,
4
5 2 h, 6 h, 14 h, 24 h and 48 h, leading always to massive cementite layers on ferrite substrates
6
7 [8, 10] (cf. Fig. 1). For these experiments “thick-plate” specimens with a thickness of 1 mm,
8
9 produced as described above, were used. In fact, the 783 K and 843 K specimens are among
10
11 those used in Ref. [10] to analyse the cementite-layer growth kinetics at the corresponding
12
13 temperatures.
14
15

16
17 Gaseous *nitriding* experiments were performed at 823 K using different NH_3/H_2 -
18
19 containing gas atmospheres yielding different nitriding potentials¹ (cf. Table 1). The applied
20
21 experimental conditions ensured the formation of compound-layer free specimens in
22
23 accordance with the Lehrer diagram [19]. Gaseous *nitriding* was performed for 42 h in order
24
25 that the ferrite substrates were saturated with interstitial nitrogen with respect to the nitriding
26
27 gas atmosphere. For these experiments “thin-plate” specimens with a thickness of 0.1 mm,
28
29 produced as described above, were used.
30
31
32
33
34
35

36 2.2 Microstructural and hardness analysis

37
38 The specimens after both the *nitriding* and the *nitrocarburising* experiments were cut into
39
40 four pieces, used for optical microscopy, hardness measurements, carrier-gas hot extraction
41
42 and X-ray diffraction (XRD), respectively.
43
44

45
46 For optical microscopy of and hardness measurements on specimen cross sections, the
47
48 nitrocarburised specimens were covered with an electrodeposited protective nickel layer using
49
50 a Watts bath [6, 20] at 333 K. The protective nickel layer avoids mechanical damage at the
51
52 surface of the metallographic cross sections and guarantees the required sharpness at the
53
54 sample surface in the cross sections. All specimens (nitriding and nitrocarburising
55
56 experiments) were embedded using a Struers LaboPress 3. Embedding was performed with 15
57
58
59
60

of $\text{NH}_3/\text{H}_2/\text{CO}/\text{N}_2$ is (hypothetically) infinite [8] although an “effective” carburising potential acts at the
specimen surface [10].

1
2
3 ml Polyfast (Buehler GmbH), a load of 15 kN, an annealing time of 5 min at 453 K and a
4
5 cooling time of 3 min down to room temperature. After embedding, the specimens were
6
7 ground, polished (final stage 1 μm diamond suspension) and etched using 1 vol.-% Nital
8
9 containing 0.1 vol.-% HCl [21]. In order to differentiate between the massive cementite layer
10
11 and the ferrite substrate, the cross-sectional specimens were stained using either (i) an alkaline
12
13 potassium permanganate solution (1 g NaOH, 1 g KOH and 4 g KMnO_4 per 100 ml distilled
14
15 water) at 328 K [8, 22] of which the effect is similar to that of a Murakami solution [6, 22] or
16
17 (ii) an alkaline sodium picrate solution (25 g NaOH and 2 g picric acid per 75 ml distilled
18
19 water) at room temperature [22]. In both cases the massive cementite layer gets, due to its
20
21 high carbon content, severely stained. The ferrite substrate remains unstained and can
22
23 therefore easily be distinguished from the cementite layer upon optical microscopy (Zeiss
24
25 Axiophot microscope). By this type of staining it is also possible to differentiate between
26
27 different nitride, carbonitride and carbide phases (also supported by electron back-scatter
28
29 diffraction) in the compound layers, see e.g. Ref. 11, indicating that in the present work
30
31 indeed were of pure cementite.
32
33
34
35
36
37

38
39 Hardness measurements (micro-Vickers) were performed with a Leica VMHT MOT
40
41 microhardness indenter using a load of 25 gf ($\cong 0.245$ N) for 10 s. Hardness-depth profile
42
43 measurements in the ferrite substrates were performed for all specimens of the
44
45 *nitrocarburising* experiments. Hardness indents were set in the ferrite substrate at selected
46
47 distances from the interface cementite/ferrite until the middle of the specimen was reached.
48
49 The exact distance values of the hardness indents from the interface cementite/ferrite were
50
51 determined by optical microscopy using the software “analySIS” (Soft Imaging System
52
53 GmbH). For each specific distance value from the interface cementite/ferrite five hardness
54
55 measurements were made; the average value was taken as the local hardness and the standard
56
57 deviation was taken as indication of the experimental error. For all specimens of the *nitriding*
58
59 experiments, which should have – due to the small specimen thickness and due to the long
60

1
2
3 treatment time – a homogeneous nitrogen content, 10 hardness measurements were made
4
5 across the cross-sectional specimen; their average value and their standard deviation was
6
7 calculated.
8
9

10 In order to relate the hardness of the ferrite substrate with its nitrogen content, values for
11 both quantities were determined for a couple of specimens with homogeneous nitrogen
12 contents in the ferrite (see section 3). The nitrogen contents of all the *nitrided* specimens
13 (compound-layer free) were determined by carrier-gas hot extraction. The same procedure
14 was applied to specimens, which were *nitrocarburised* at 823 K with a treatment time of 6 h,
15 14 h, 24 h and 48 h, since these specimens do *not* exhibit a nitrogen concentration (hardness)
16 gradient across the ferrite substrate in the cross section (cf. Fig. 2b). Prior to nitrogen-content
17 determination by carrier-gas hot extraction on the nitrocarburised specimens, the massive
18 cementite layer was removed by grinding so that only the nitrogen-enriched substrate was
19 analysed. After completion of the grinding procedure, it was checked by X-ray diffraction
20 whether the entire cementite layer had been removed.
21
22
23
24
25
26
27
28
29
30
31
32
33
34
35

36 To additionally verify the presence or absence of a (cementite) compound layer and of
37 the possible presence of other nitride and carbonitride phases, phase identification was carried
38 out by X-ray diffractometry. A PANalytical X'Pert Multi-Purpose Diffractometer, which was
39 equipped with a graphite monochromator in the diffracted beam, was used. The diffractometer
40 was operated with CoK α radiation in Bragg-Brentano geometry. Each specimen was rotated
41 around its surface normal during the measurements to achieve better crystallite statistics.
42
43
44
45
46
47
48
49
50
51
52

53 **3. Experimental results and evaluation: hardness measurements and nitrogen-** 54 **content determination** 55 56

57 Each *nitrocarburising* experiment performed at 783 K, 823 K and 843 K led to the formation
58 of a massive cementite layer on the ferrite substrates (cf. Fig. 1) [8,10]. The cementite layers
59 exhibit a characteristic microstructure (partially rough ferrite-cementite interface) and a
60

specific orientation relationship with the ferrite substrate [12]. After cross-sectional metallographic preparation, hardness-depth profile measurements were performed in the ferrite substrate (cf. Figs. 2a - 2c).

In order to transform hardness-depth profiles into nitrogen concentration-depth profiles (cf. Figs. 2a – 2c), the dependence of hardness on nitrogen content in ferrite has to be known. Such a dependence was obtained on the basis of the results for hardness and nitrogen content in homogeneously nitrided/nitrocarburised ferrite given in Table 1 and shown in Fig. 3.

Table 1: The experimentally determined (average) hardness values and (average) nitrogen contents (results from carrier-gas extraction) of all *nitrided* specimens. Composition (NH₃ and H₂ contents and corresponding nitriding potential) of the *nitriding* gas atmosphere, yielding compound-layer free specimens, have been indicated. The experiments were performed for 42 h at 823 K leading to a homogeneous solid solution of interstitial nitrogen in the ferrite substrate. The hardness of pure iron without any nitrogen dissolved determined in this work equals 100 ± 2 HV. Similar results obtained for some selected (see text) *nitrocarburising* experiments at 823 K have been given as well.

nitriding experiments

NH ₃ content [vol.-%]	2	4	6	7	9	12	13
H ₂ content [vol.-%]	98	96	94	93	91	88	87
nitriding potential, r_N [atm ^{-1/2}]	0.02	0.04	0.06	0.08	0.1	0.14	0.16
hardness [HV]	116 ± 7	119 ± 4	133 ± 6	147 ± 3	152 ± 3	182 ± 9	205 ± 7
nitrogen concentration [at.-%]	0.034	0.075	0.108	0.144	0.184	0.297	0.367

nitrocarburising experiments

treatment time [h]	6	14	24	48
hardness [HV]	147 ± 4	158 ± 2	171 ± 2	194 ± 3
nitrogen concentration [at.-%]	0.136	0.176	0.228	0.307

It follows that a linear dependence exists between nitrogen content and hardness of the ferrite substrate:

$$C_N^{\alpha\text{-Fe}} = mh + b, \quad (1)$$

where $C_N^{\alpha\text{-Fe}}$ denotes the nitrogen concentration in the ferrite substrate, and h its hardness. Least-squares fitting of a straight line to the experimental data in Fig. 3 yielded the following values for m (slope of the straight line in Fig. 3) and b (part cut from the ordinate): $m = (3.46 \pm 0.1) \cdot 10^{-3} \frac{\text{at.-%}}{\text{HV}}$ and $b = -0.354 \pm 0.02 \text{ at.-%}$. On this basis, the experimentally determined hardness-depth profiles can be transformed into nitrogen concentration-depth profiles (cf. Figs. 2a – 2c). This was done for all considered treatment temperatures (783 K, 823 K and 843 K) and treatment times.

Such quantitative information on the nitrogen concentration in ferrite cannot be obtained by other techniques. Whereas e.g. carrier-gas hot extraction can only provide an average nitrogen concentration across the whole specimen (instead of a location-resolved nitrogen concentration), the sensitivity of electron probe microanalysis (EPMA) is too low for the presently determined nitrogen concentrations.

4. Modelling nitrogen concentration-depth profile development

4.1 General assumptions

The experimentally determined nitrogen concentration-depth profiles will be simulated to analyse, on the basis of comparison with the experimentally determined nitrogen concentration-depth profiles, the diffusivity of nitrogen through cementite.

Consider a laterally infinitely extended iron plate of finite thickness. Nitrogen can enter this plate from both sides; a symmetrical (with respect to the centre plane of the plate) nitrogen concentration-depth profile is built up.

The process of gaseous nitrocarburising can be subdivided into four different steps: (i) diffusion of ammonia from the gas phase to the surface of the specimen, (ii) dissociation of ammonia at the surface, (iii) nitrogen diffusion through the growing cementite layer of time-dependent thickness, (iv) nitrogen diffusion within ferrite (after having diffused through the cementite layer) from the interface cementite/ferrite to the core of the specimen. Ad (i): In the present experiments the gas-flow through the quartz-tube furnace is large; the gas composition at the sample surface can be taken constant for a constant treatment temperature [10]. Ad (ii): Already after very short treatment time dissociation of ammonia at the surface of the specimen is *not* rate determining for the nitrogen uptake; instead nitrogen diffusion through the growing cementite layer is rate-determining (in contrast with the case of nitriding pure ferrite [23]). The conditions indicated under ad (i) and ad (ii) imply that local equilibrium prevails at the interface of the gas atmosphere and the specimen. Furthermore, local equilibrium is assumed to hold at the interface cementite/ferrite, which in the present context in particular implies that there is no chemical-potential gradient for nitrogen at that interface.

Nitrogen diffusion within ferrite is governed by Fick's second law

$$\frac{\partial C_N^{\alpha\text{-Fe}}}{\partial t} = D_N^{\alpha\text{-Fe}} \frac{\partial^2 C_N^{\alpha\text{-Fe}}}{\partial x^2}, \quad (2)$$

where $D_N^{\alpha\text{-Fe}}$ is the diffusion coefficient of nitrogen in ferrite (taken as concentration independent), $C_N^{\alpha\text{-Fe}}$ the nitrogen concentration at depth x (measured from the interface cementite/ferrite²) and t the time of diffusion.

The flux of nitrogen through cementite at the interface cementite/ferrite, $J_N^{\text{Fe}_3\text{C}}|_{x=0}$, differs from the flux of nitrogen into ferrite at this interface $J_N^{\alpha\text{-Fe}}|_{x=0}$ by a term considering the amount of N consumed by the moving interface cementite/ferrite due to the concentration difference at the interface:

$$\begin{aligned} J_N^{\text{Fe}_3\text{C}}|_{x=0} &= J_N^{\alpha\text{-Fe}}|_{x=0} + \left(C_{\text{N,interface}}^{\text{Fe}_3\text{C}} - C_{\text{N,interface}}^{\alpha} \right) \frac{dS_{\text{Fe}_3\text{C}}}{dt} \\ &= -D_N^{\alpha\text{-Fe}} \frac{\partial C_N^{\alpha\text{-Fe}}}{\partial x} \Big|_{x=0} + \left(C_{\text{N,interface}}^{\text{Fe}_3\text{C}} - C_{\text{N,interface}}^{\alpha} \right) \frac{dS_{\text{Fe}_3\text{C}}}{dt}, \end{aligned} \quad (3)$$

² The cementite layer is thin compared to the ferrite substrate at all considered treatment times and the cementite layer grows much slower than the extent of the nitrogen concentration-depth profile in the substrate. Therefore, the consumption of a part of the ferrite upon formation of the cementite is neglected in the modelling of the diffusion of nitrogen in ferrite.

where $x = 0$ denotes the location coordinate which represents the interface cementite/ferrite. There are no reliable data about the N content in cementite (it is even unclear whether the concentration difference in Eq. (3) should be positive or negative). However, test calculations with nitrogen contents in cementite ranging from 0 at.% to 0.5 at. % indicate that – given the known growth rate of cementite – the nitrogen consumption or release due to the growing cementite (at the cost of ferrite with a nitrogen content of $C_{N,interface}^{\alpha-Fe}$) is negligible compared to the overall nitrogen flux through the cementite layer.

Nitrogen enters the ferrite substrate at both sides. Hence, a symmetrical nitrogen concentration-depth profile results and no net flux of nitrogen through the middle of the sample occurs, leading to the second boundary condition

$$\left. \frac{\partial C_N^{\alpha-Fe}}{\partial x} \right|_{x=Z} = 0, \quad (4)$$

where $x = Z$ denotes the position of the centre plane.

Before nitrogen can pass the interface cementite/ferrite and can diffuse through ferrite, it must be transported through the cementite layer. Nitrogen diffusion through cementite is provoked by a gradient of the chemical potential of nitrogen across the cementite layer (cf. Fig. 4)

$$F = - \left(\frac{\partial \mu_N^{Fe_3C}}{\partial x} \right)_{p,T}, \quad (5)$$

where F is the thermodynamic force, $\mu_N^{Fe_3C}$ the chemical potential of nitrogen in cementite and x the location coordinate, T the treatment temperature and p the pressure.

For the nitrogen flux through cementite, $J_N^{\text{Fe}_3\text{C}}$, it holds that [24]

$$\begin{aligned} J_N^{\text{Fe}_3\text{C}} &= v_N^{\text{Fe}_3\text{C}} C_N^{\text{Fe}_3\text{C}} = M_N^{\text{Fe}_3\text{C}} F C_N^{\text{Fe}_3\text{C}} \\ &= -M_N^{\text{Fe}_3\text{C}} C_N^{\text{Fe}_3\text{C}} \left(\frac{\partial \mu_N^{\text{Fe}_3\text{C}}}{\partial x} \right)_{p,T} = -D_N^{\text{Fe}_3\text{C}} \left(\frac{\partial C_N^{\text{Fe}_3\text{C}}}{\partial x} \right)_{p,T}, \end{aligned} \quad (6)$$

where $v_N^{\text{Fe}_3\text{C}}$ denotes the drift velocity of nitrogen in cementite, $M_N^{\text{Fe}_3\text{C}}$ is the mobility of nitrogen in cementite, $D_N^{\text{Fe}_3\text{C}}$ represents the diffusion coefficient of nitrogen in cementite and $C_N^{\text{Fe}_3\text{C}}$ is the nitrogen concentration in cementite. The diffusion coefficient of nitrogen in cementite can be expressed by

$$D_N^{\text{Fe}_3\text{C}} = M_N^{\text{Fe}_3\text{C}} RT \left(1 + \frac{\partial \ln \gamma_N^{\text{Fe}_3\text{C}}}{\partial \ln C_N^{\text{Fe}_3\text{C}}} \right), \quad (7)$$

where $\left(1 + \frac{\partial \ln \gamma_N^{\text{Fe}_3\text{C}}}{\partial \ln C_N^{\text{Fe}_3\text{C}}} \right)$ is the thermodynamic factor, with $\gamma_N^{\text{Fe}_3\text{C}}$ as the activity coefficient of nitrogen in cementite. The solubility of nitrogen in cementite is extremely small, e.g. for 1593 K a solubility of about 0.064 at.-% was reported [25]. Due to this extremely limited solubility, Henry's law [26, 27] is assumed for nitrogen in cementite. Consequently, the thermodynamic factor equals one and $D_N^{\text{Fe}_3\text{C}}$ reduces to

$$D_N^{\text{Fe}_3\text{C}} = M_N^{\text{Fe}_3\text{C}} RT = D_N^{*,\text{Fe}_3\text{C}}, \quad (8)$$

where $D_N^{*,\text{Fe}_3\text{C}}$ is the (tracer-)diffusion coefficient of nitrogen in cementite. Thus,

$$J_N^{\text{Fe}_3\text{C}} = -D_N^{*,\text{Fe}_3\text{C}} \left(\frac{\partial C_N^{\text{Fe}_3\text{C}}}{\partial x} \right)_{p,T} . \quad (6b)$$

A linear concentration profile of nitrogen across cementite is assumed in Eq. (6b). The concentration difference of nitrogen across the cementite layer is given by the difference of the nitrogen concentration in cementite at the interface gas atmosphere/cementite, $C_{N,\text{surface}}^{\text{Fe}_3\text{C}}$, and the nitrogen concentration in cementite at the interface cementite/ferrite, $C_{N,\text{interface}}^{\text{Fe}_3\text{C}}$. Then Eq. (6b) can be given as

$$J_N^{\text{Fe}_3\text{C}} = \frac{D_N^{*,\text{Fe}_3\text{C}} (C_{N,\text{surface}}^{\text{Fe}_3\text{C}} - C_{N,\text{interface}}^{\text{Fe}_3\text{C}})}{S_{\text{Fe}_3\text{C}}} , \quad (9)$$

where $S_{\text{Fe}_3\text{C}}$ is the cementite-layer thickness.

The nitrogen concentrations in cementite at both interfaces (gas atmosphere/cementite and at the interface cementite/ferrite) will be expressed in terms of “corresponding” (see what follows) nitrogen concentrations in ferrite. For both, cementite and ferrite, Henry’s law can be adopted. Therefore, for cementite and ferrite in (hypothetical) equilibrium with each other and, possibly additionally, with the same outer gas atmosphere, the concentrations of nitrogen in cementite, $C_N^{\text{Fe}_3\text{C}}$, and in ferrite, $C_N^{\alpha\text{-Fe}}$, are in equilibrium related by³

³ For the chemical potential of nitrogen in cementite it holds that $\mu_N^{\text{Fe}_3\text{C}} = \mu_N^0 + RT \ln \gamma_N^{\text{Fe}_3\text{C}} x_N^{\text{Fe}_3\text{C}}$ and for the chemical potential of nitrogen in ferrite it holds that $\mu_N^{\alpha\text{-Fe}} = \mu_N^0 + RT \ln \gamma_N^{\alpha\text{-Fe}} x_N^{\alpha\text{-Fe}}$. Assuming for both, cementite and ferrite, the same reference state and Henry’s law (constant activity coefficient of nitrogen), the mole fractions of nitrogen in cementite and ferrite in equilibrium with each other are related by a partition

$$C_N^{\text{Fe}_3\text{C}} = \varphi C_N^{\alpha\text{-Fe}}, \quad (10)$$

where φ is the partition coefficient. Hence, the nitrogen concentration in ferrite at the cementite/ferrite interface in (real, local) equilibrium with cementite at the same interface corresponds to $C_{N,\text{interface}}^{\alpha\text{-Fe}} = C_{N,\text{interface}}^{\text{Fe}_3\text{C}} / \varphi$ and thus $C_{N,\text{interface}}^{\text{Fe}_3\text{C}} = \varphi C_{N,\text{interface}}^{\alpha\text{-Fe}}$. Diffusion of nitrogen through the cementite will come to a halt if the nitrogen concentration in the ferrite corresponds to the nitrogen concentration which would prevail in ferrite in (hypothetical) equilibrium with the gas atmosphere, $C_{N,\text{eq}}^{\alpha\text{-Fe}}$. Hence, the concentration of nitrogen in cementite at the surface in (real, local) equilibrium with the gas atmosphere, $C_{N,\text{surface}}^{\text{Fe}_3\text{C}}$, is given by $C_{N,\text{surface}}^{\text{Fe}_3\text{C}} = \varphi C_{N,\text{eq}}^{\alpha\text{-Fe}}$.

The above consideration implies that Eq. (9) can be written as

$$J_N^{\text{Fe}_3\text{C}} = \frac{\varphi D_N^{*\text{Fe}_3\text{C}} (C_{N,\text{eq}}^{\alpha\text{-Fe}} - C_{N,\text{interface}}^{\alpha\text{-Fe}})}{S_{\text{Fe}_3\text{C}}}, \quad (11)$$

The cementite-layer thickness $S_{\text{Fe}_3\text{C}}$ has been determined experimentally for the present samples. The layer thickness could be described for each temperature by adopting a modified parabolic growth law [8, 10]

$$S_{\text{Fe}_3\text{C}}^2(t) = k(T)t + S_0^2(T), \quad (12)$$

coefficient, φ , according to $\varphi = \frac{\gamma_N^{\alpha\text{-Fe}}}{\gamma_N^{\text{Fe}_3\text{C}}}$. It will be assumed that for the minute range of nitrogen concentration in cementite φ does not depend on nitrogen concentration.

where k denotes the parabolic growth constant for cementite and S_0 a (hypothetical) initial cementite-layer thickness at $t = 0$ (see discussion in Ref. [8]). Combining Eqs. (11) and (12)

leads to
$$J_N^{\text{Fe}_3\text{C}} = \frac{\varphi D_N^{*,\text{Fe}_3\text{C}} (C_{\text{N,eq}}^{\alpha\text{-Fe}} - C_{\text{N,interface}}^{\alpha\text{-Fe}})}{(kt + S_0^2)^{1/2}} .$$

4.2 Simulation of nitrogen concentration-depth profiles; numerical procedure

For the simulation of the nitrogen concentration-depth profiles, Fick's first and second law have to be solved subject to the boundary conditions given by Eqs. (3) and (4). This can be done numerically on the basis of the method after Crank and Nicolson [23, 28] using the implicit finite-difference method. For that purpose the nitrogen concentration profile within ferrite was calculated for equidistant grid points in space (distance Δx) (cf. Fig. 4) at different time steps (see what follows in section 5). Details of the numerical procedure are described in supplementary material published together with the online version.

5. Results of the simulation

The simulation was performed with $M = 100$ grid points (up to the middle of the specimen) and different time steps. The increment of time was increased by 0.5 % after each generation of a nitrogen concentration profile [23], recognising the decrease of the nitrogen-concentration gradients with time, in order to reduce calculation time. Doing this, the condition $r = \frac{D_N^{*,\text{Fe}_3\text{C}} \Delta t}{(\Delta x)^2} \leq 1/2$ has to be fulfilled [28], where Δt denotes the increment of the

time and Δx denotes the grid-point distance. The simulation was started at the respective treatment temperatures on the basis of the nitrogen concentration-depth profile determined after 6 h, since for smaller treatment times the diffusion geometry and mechanism is incompatible with the model (see section 6.2).

The following parameters were known: (i) the diffusion coefficient of nitrogen in ferrite, which was calculated for the respective treatment temperature according to Ref. [29] (cf. Table 2) and (ii) the cementite-layer thickness, which was determined experimentally. Hence, the fitting parameters were: the equilibrium nitrogen concentration in ferrite, $C_{N,eq}^{\alpha-Fe}(T)$, and the product of the partition coefficient and the (tracer-)diffusion coefficient of nitrogen in cementite, $\phi D_N^{*,Fe_3C}$. Values for these parameters were determined (for each considered treatment temperature) by minimising the sum of the squared differences of simulated and experimental nitrogen concentrations for all treatment times *simultaneously* (cf. Figs. 2a – 2c). The results obtained for $C_{N,eq}^{\alpha-Fe}$ and $\phi D_N^{*,Fe_3C}$ have been gathered in Table 2 and Fig. 5.

Table 2: Results of the simulation of nitrogen concentration-depth profiles. The equilibrium nitrogen concentration in ferrite, and the product of the partition coefficient and the (tracer-)diffusion coefficient of nitrogen through cementite were refined by matching of the simulated data and the experimental data by least-squares fitting. Furthermore, the diffusion coefficient of nitrogen in ferrite has been given according to Ref. [29].

treatment temperature, T	783	823	843
[K]			
equilibrium nitrogen concentration in ferrite, $C_{N,eq}^{\alpha-Fe}$	0.599	0.613	0.700
[at.-%]			
product of the partition coefficient and the (tracer-)diffusion coefficient of nitrogen through cementite, $\phi D_N^{*,Fe_3C}$ [m ² /s]	$2.9 \cdot 10^{-15}$	$4.8 \cdot 10^{-15}$	$5.9 \cdot 10^{-15}$

diffusion coefficient of nitrogen in ferrite, $D_N^{\alpha\text{-Fe}}$

$$7.4 \cdot 10^{-12} \quad 1.3 \cdot 10^{-11} \quad 1.8 \cdot 10^{-11}$$

[m²/s]

Adopting an Arrhenius-type temperature dependence for the (tracer-)diffusion coefficient of nitrogen in cementite and taken the partition coefficient φ as temperature independent, a plot of the logarithm of $\varphi D_N^{*\text{Fe}_3\text{C}}$ vs. $1/T$ should yield a straight line. This is observed indeed; see Fig. 5. The slope of the straight line obtained equals $-Q/R$, with Q as the activation energy of nitrogen diffusion in cementite and R as the gas constant. It follows: $Q = 65 \pm 2$ kJ/mol.

6. Concluding discussion

6.1 Hardness/concentration-depth profiles

The hardness of the ferrite substrates increases linearly with the nitrogen concentration. Upon embedding (cf. section 2), which has to be considered as a heat treatment, the nitrogen in the ferrite forms (semi-)coherent $\alpha''\text{-Fe}_{16}\text{N}_2$ precipitates [30-34], which are responsible for the hardness increase as measured at room temperature. In order to guarantee comparability of the hardness measurements, the embedding has to be performed in a reproducible way. Therefore, a special standard embedding procedure was developed, which has been described in section 2.

In the course of relating the ferrite hardness with the nitrogen content in the ferrite, the effect of present carbon was neglected. The amount of carbon which can be dissolved in ferrite at 823 K is more than twenty times smaller than the amount of nitrogen (see introduction). Already because of this recognition it is expected that a much smaller

1
2
3 hardening effect due to carbides in ferrite is expected than due to nitrides. Indeed, for carbon
4 in ferrite an increase of Vickers hardness of at maximum of 15 HV was observed in Ref. [35],
5
6 which is much less than the maximum increase of 100 HV observed for nitrogen in ferrite (cf.
7
8 Figure 3). Moreover, in Ref. [35] the solid solution treatment prior to the age hardening was
9
10 performed at temperatures as high 973 K, which certainly led to dissolution of more carbon in
11
12 the ferrite than in the present experiments conducted at ≤ 843 K. Thus the (maximum
13
14 possible) hardening effect due to carbon in ferrite in the present work is expected to be even
15
16 smaller than 15 HV. Further, the data points in Figure 3 do not differ systematically from the
17
18 common straight line, independently of whether the points originate from a nitrocarburised
19
20 specimen (containing some carbon in the ferrite) or from purely nitrated specimen (containing
21
22 no carbon in the ferrite), confirming that the hardness depends practically only on the nitrogen
23
24 content in the ferrite.
25
26
27
28
29
30

31
32 Moreover, it must be noted that the calibration line shown in Fig. 3 was determined on
33
34 the basis of experiments performed at 823 K. This calibration line was also applied to the data
35
36 obtained at 783 K and 843. The true relation between hardness and nitrogen content at 783 K
37
38 and 843 K may differ slightly from that pertaining at 823 K. This may be the origin of the
39
40 slightly negative nitrogen-concentration values in the ferrite substrate for some data points at
41
42 very short treatment times (0.5 h and 2 h) at 783 K (cf. Fig. 2a).
43
44
45

46 The data obtained for the nitrogen concentration-depth profiles at the three different
47
48 considered treatment temperatures indicate pronounced nitrogen concentration gradients in
49
50 the ferrite matrix at short treatment times as 0.5 h and 2 h; the concentration gradients level
51
52 off with increasing treatment time. The development of the nitrogen concentration-depth
53
54 profile in the ferrite substrate is dominated by two processes: (i) nitrogen transport through
55
56 the cementite layer via diffusion. The cementite-layer thickness increases as a function of the
57
58 treatment time (according to a modified parabolic growth law [8, 10]). Therefore, the nitrogen
59
60 flux through cementite *decreases* with *increasing* treatment time. (ii) The inward-diffusion of

nitrogen into the ferrite substrate remains relatively fast. From (i) and (ii) it is concluded that the initially large nitrogen concentration gradient in the ferrite substrate decreases with time, as observed.

6.2 Simulation of nitrogen concentration-depth profiles

In the present work, nitrogen concentration-depth profiles in the ferrite substrate with a growing cementite layer at the surface were simulated. In the literature [23] such an approach was already applied for the calculation of nitrogen concentration-depth profiles of compound-layer free ferrite specimens. In that case local equilibrium between gas atmosphere and the surface of the specimen was not immediately established. Therefore, nitrogen absorption and/or ammonia dissociation and nitrogen transfer through the surface contributed significantly to the process kinetics. In fact, nitrogen transfer through the cementite layer in the present case and nitrogen transfer through the surface in case of nitriding ferrite without compound layer at the surface (Ref. [23]) can be conceived as analogues. However, different dependences on $(C_{N,eq}^{\alpha-Fe} - C_{N,interface}^{\alpha-Fe})$ occur in both cases: In Ref. [23]:

$$J_N^{surf} \propto k(C_{N,eq}^{\alpha-Fe} - C_{N,interface}^{\alpha-Fe}) \text{ and here: } J_N^{Fe_3C} \propto \frac{D_N^{*Fe_3C}(C_{N,eq}^{\alpha-Fe} - C_{N,interface}^{\alpha-Fe})}{S_{Fe_3C}}, \text{ i.e. in the present, last case an}$$

extra time dependence, through S^{Fe_3C} , is introduced.

Treatment times of 0.5 h and 2 h were not considered in the simulation procedure. In the early stage of cementite formation ($t < 6$ h), cementite-layer growth proceeded faster than as predicted by the developed model. This can be explained as follows: (i) in the early stage of cementite formation an incompletely closed cementite layer is present [8,10]. Nitrogen diffusion from the surface of the specimen into ferrite proceeds directly, i.e. bypassing cementite⁴. (ii) Further, just after the formation of a closed cementite layer, short-circuit diffusion of nitrogen through thin and defect-rich parts of the cementite layer occurs. In this stage of cementite formation, cementite is expected to exhibit a relatively high grain-boundary

⁴ Transport of nitrogen in ferrite is much faster than transport of nitrogen through cementite.

1
2
3 density; for data demonstrating grain-boundary diffusion in cementite, see Ref. [12]. Due to
4
5 such a ‘bypass/short-circuit’ mechanism, nitrogen can be transported relatively fast through
6
7 the cementite layer in the early stage of cementite formation⁵. Therefore, treatment times < 6
8
9 h were not used in the data evaluation on the basis of the model developed in section 4.1.
10
11

12 Literature data for the equilibrium nitrogen concentration in ferrite vary considerably:
13
14 e.g. the values reported in Ref. [36] are distinctly lower than the values reported in Ref. [17].
15
16 The values of $C_{N,eq}^{\alpha-Fe}$ obtained in the present work are generally larger than those compatible
17
18 with the data from Refs. [17] and [36]. These differences can be understood recognising that
19
20 the nitrogen concentration in the ferrite substrate, $C_{N,eq}^{\alpha-Fe}$, as determined in the present work,
21
22 pertains to the (hypothetical) equilibrium of ferrite with the present nitrocarburising gas
23
24 atmosphere. In reality such an equilibrium cannot occur: for such high nitrogen
25
26 concentrations, solubility limits for nitrogen in ferrite in equilibrium with iron (carbo-)nitrides
27
28 are surpassed, and formation of γ' -Fe₄N below 833 K or of ϵ -Fe₃(N,C)_{1+x} above 843 K [11]
29
30 occurs. Indeed, in the present work, treatment times \gg 48 h at 853 K occasionally led to the
31
32 formation of these (carbo-)nitride phases at the cementite/ferrite interface.
33
34
35
36
37
38
39

40 According to the knowledge of the present authors, diffusion data of nitrogen in
41
42 cementite have not been reported, before. The values obtained for the product of the partition
43
44 coefficient and the (tracer-)diffusion coefficient of nitrogen through cementite are
45
46 considerably lower than values for the diffusion coefficients of nitrogen in ferrite [29, 37] (cf.
47
48 Table 2) and iron nitrides [38-41] at similar treatment temperatures. The role of the cementite
49
50 layer as diffusion barrier for nitrogen can be illustrated by assuming that the cementite layer
51
52 would instead consist of ferrite. In that case, in Eq. (11) $\phi D_N^{*,Fe_3C}$ should be substituted by
53
54 $D_N^{\alpha-Fe}$. Hence, the nitrogen flux through the (cementite) surface layer, $J_N^{Fe_3C}$, would increase
55
56
57
58
59
60

⁵ A similar explanation was used for the observed enhanced initial growth rate during carbon-diffusion controlled cementite-layer growth on ferrite [8,10].

1
2
3
4 by a factor $D_N^{\alpha\text{-Fe}} / \varphi D_N^{*\text{Fe}_3\text{C}}$, i.e. a factor of about 2500 - 3000 (cf. Table 2). This clearly
5
6 demonstrates the diffusion-barrier behaviour of the cementite layer for nitrogen, which then
7
8 could be due in particular to the very low solubility of nitrogen in cementite, leading to very
9
10 small values of φ ; further, the pre-exponential factors contained in $D_N^{\alpha\text{-Fe}}$ and $D_N^{*\text{Fe}_3\text{C}}$ may
11
12 differ considerably.
13
14

15
16 The activation energy of nitrogen diffusion through cementite (here determined as $65 \pm$
17
18 2 kJ/mol) is relatively low as compared to real or “apparent” activation energies for carbon
19
20 diffusion through cementite which are in the range of 110 – 185 kJ/mol [10, 42-44], and for
21
22 nitrogen diffusion in iron nitrides, which are in the range of 92 – 144 kJ/mol [40, 41, 45]. The
23
24 activation energy for nitrogen diffusion in cementite appears to be as low as the activation
25
26 energy for nitrogen (or carbon) diffusion in ferrite, which is about 78 – 79 kJ/mol [29, 37].
27
28 One possibility is that φ , although very small, depends significantly on temperature and thus
29
30 affects the activation energy value determined. Another possibility is that the low activation
31
32 energy for $D_N^{*\text{Fe}_3\text{C}}$ may hint at nitrogen transport favourably occurring via cementite grain
33
34 boundaries; preferred diffusion of carbon along grain boundaries in cementite was reported
35
36 very recently [12]. A role of defects (which later-on heal out) has indeed already been
37
38 discussed above for the initial fast stage of nitrogen transport through cementite (see
39
40 paragraph 2 of the present section 6.2), but it is imaginable that still later nitrogen diffusion
41
42 along remaining grain boundaries (or other extended defects) may contribute to the occurring
43
44 nitrogen flux through cementite. As long as the grain-boundary density remains constant, the
45
46 grain boundaries’ contribution to the nitrogen transport will lead to same kinetic equations as
47
48 derived in section 4, and the obtained diffusion coefficient becomes an “effective” diffusion
49
50 coefficient and the activation energy is an “effective” activation energy [46].
51
52
53
54
55
56
57
58
59
60

7. Conclusions

- 1
2
3
4
5
6
7
8
9
10
11
12
13
14
15
16
17
18
19
20
21
22
23
24
25
26
27
28
29
30
31
32
33
34
35
36
37
38
39
40
41
42
43
44
45
46
47
48
49
50
51
52
53
54
55
56
57
58
59
60
- (i) Hardness-depth profile measurements provide a suitable method to quantitatively determine nitrogen-concentration depth profiles in ferrite (maximal nitrogen content: ≈ 0.4 at.-%) after well-defined thermal post-treatment on the basis of a calibration. The relation between hardness and nitrogen content was found to be linear.
 - (ii) Massive cementite layers with a time-dependent thickness can be generated on ferrite substrates by gaseous nitrocarburising at 783 K, 813 K and 843 K. The nitrogen concentration-depth profile in the ferrite substrate underneath the growing cementite layer can be simulated on the basis of a developed model using the implicit finite-difference method, yielding values for the diffusivity of nitrogen through cementite.
 - (iii) The effective activation energy of nitrogen diffusion through cementite is about as large as the activation energy of nitrogen diffusion in ferrite. This may hint at nitrogen grain-boundary diffusion as dominant transport mechanism of nitrogen through cementite. The cementite layer acts as a diffusion barrier for nitrogen in particular because of the very low solubility of nitrogen in cementite.

References

- [1] P. M. Unterweiser and A.G. Gray, editors: Source Book on Nitriding. ASM, Metals Park, OH, (USA), 1977.
- [2] D. Liedtke, U. Baudis, J. Boßlet, U. Huchel, H. Klümper-Westkamp, W. Lerche and H.-J. Spieß H-J: Wärmebehandlung von Eisenwerkstoffen – Nitrieren und Nitrocarburieren. Expert-Verlag, Renningen-Malmsheim (Germany), 2006.
- [3] T.B. Massalski and H. Okamoto, editors: Binary Alloy Phase Diagrams, ASM International, Metals Park, OH (USA), 1990.
- [4] H. Du and M. Hillert: Z. Metallkde., 1991, vol. 82, pp. 310-316.
- [5] C.H. Knerr, T.C. Rose, J.H. Filkowski. In: J.R. Davis, G.M. Davidson, S.R. Lampman, T.B. Zorc, J.L. Daquila, A.W. Ronke, et al., editors: ASM Handbook, vol. 4, Heat Treating, ASM International, Metals Park, OH (USA), 1991, pp. 387-409.
- [6] P.F. Colijn, E.J. Mittemeijer and H.C.F. Rozendaal: Z. Metallkde., 1983, vol. 74, pp. 620-627.
- [7] M. A. J. Somers and E. J. Mittemeijer: Surf. Eng., 1987, vol. 3, pp. 123-137.
- [8] T. Gressmann, M. Nikolussi, A. Leineweber and E.J. Mittemeijer: Scr. Mat., 2006; vol. 55, pp. 723-726.
- [9] E.J. Mittemeijer: J. Heat Treating, 1983, vol. 3, pp. 114-119.
- [10] M. Nikolussi, A. Leineweber and E.J. Mittemeijer: J. Mater. Sci., 2009, vol. 44, pp. 770-777.
- [11] M. Nikolussi, A. Leineweber and E.J. Mittemeijer: Int. J. Mat. Res., 2007, vol. 98, pp. 1086-1092.
- [12] M. Nikolussi, A. Leineweber and E.J. Mittemeijer: Acta Mat., 2008, vol. 56, pp. 5837-5844.
- [13] A. Leineweber, T. Liapina, T. Gressmann, M. Nikolussi and E. J. Mittemeijer: *Adv. Sci. Techn.*, 2006, 46, 32-41.

- 1
2
3 [14] M. Nikolussi, S. Shang, T. Gressmann, A. Leineweber, E. J. Mittemeijer, Y. Wang and
4
5 Z.-K. Liu: *Scr. Mat.*, 2008, vol. 59, 814-817.
6
7
8 [15] Sone, T., Tsunasawa, E. Yamanaka, K.: *Trans. Japan Inst. Met.*, 1981 vol. 22, pp. 237-
9
10 243.
11
12 [16] A. Schneider and H. J. Grabke: *Mater. Corr.*, 2003, vol. 54, pp. 793-804.
13
14 [17] J. Kunze: *Nitrogen and Carbon in Iron and Steel*. Akademie-Verlag, Berlin (Germany),
15
16 1990.
17
18 [18] E.J. Mittemeijer and J.T. Slycke: *Surf. Eng.*, 1996, vol. 12, pp. 152-162.
19
20 [19] E. Lehrer: *Z. Elektrochem.*, 1930, vol. 36, pp. 383-392.
21
22 [20] R. Chatterjee-Fischer, R. Bodenhagen, F.-W. Eysell, R. Hoffmann, D. Liedtke, H.
23
24 Mallener, W. Rembges, A. Schreiner and G. Welker: *Wärmebehandlung von*
25
26 *Eisenwerkstoffen*. Expert-Verlag, Renningen-Malmsheim, 1995.
27
28 [21] A. Wells: *J. Mat. Sci.*, 1985, vol. 20, pp. 2439-2445.
29
30 [22] G. Petzow: *Metallographic Etching*. ASM International, Materials Park, OH (USA),
31
32 1999.
33
34 [23] H.C.F. Rozendaal, E.J. Mittemeijer, P.F. Colijn and P.J. van der Schaaf: *Metall. Trans.*
35
36 *A*, 1983, vol. 14A, pp. 395-399.
37
38 [24] P.G. Shewmon: *Diffusion in Solids*. 2nd ed., The Minerals, Metals & Materials Society
39
40 1989.
41
42 [25] A. Kagawa and T. Okamoto: *Trans. Japan Inst. Met.*, 1981, vol. 22, vol. 137-143.
43
44 [26] P.W. Atkins: *Physikalische Chemie*. Wiley-VCH, Weinheim (Germany), 2001.
45
46 [27] G. Wedler: *Lehrbuch der physikalischen Chemie*. Wiley-VCH, Weinheim (Germany)
47
48 2007.
49
50 [28] J. Crank: *The Mathematics of Diffusion*. 2nd edition, Oxford Science Publications (UK),
51
52 1975.
53
54 [29] M. Weller: *Mater. Sci. Forum*, 2001, vol. 366-368, pp. 95-137.
55
56
57
58
59
60

- 1
2
3 [30] E. Kubalek: Härtere Tech. Mitt., 1968, vol. 23, pp. 177-197.
4
5 [31] D.H. Jack and K.H. Jack: Mat. Sci. Eng., 1973, vol. 11, pp. 1-27.
6
7 [32] Y. Inokuti, N. Nishida and N. Ōhashi: Metall. Trans. A, 1975, vol. 6A, pp. 773-784.
8
9 [33] U. Dahmen, P. Ferguson and K.H. Westmacott: Acta Metall., 1987, vol. 35, pp. 1037-
10 1046.
11
12 [34] Z.Q. Liu, Y.X. Chen, Z.K. Hei, D.X. Li and H. Hashimoto: Metall. Mater. Trans. A,
13 2001, vol. 32A, pp. 2681-2688.
14
15 [35] Tsou, A. L., Nutting, J., Menter, J.W.: J. Iron Steel Inst., 1952, pp. 163-171.
16
17 [36] B.J. Kooi, M.A.J. Somers and E.J. Mittemeijer: Metall. Mater. Trans. A, 1996, vol. 27A,
18 pp. 1055-1061.
19
20 [37] J.D. Fast and M.B. Verrijb: J. Iron Steel Inst., 1954, vol. 176, pp. 24-27.
21
22 [38] K. Schwerdtfeger, P. Grieveson and E.T. Turkdogan: Trans. Metall. Soc. AIME, 1969,
23 vol. 245, pp. 2461-2466.
24
25 [39] M.A.J. Somers and E.J. Mittemeijer: Metall. Mater. Trans. A, 1995, vol. 26A, pp. 57-74.
26
27 [40] E.J. Mittemeijer and M.A.J. Somers: Surf. Eng., 1997, vol. 13, pp. 483-497.
28
29 [41] T. Liapina, A. Leineweber and E.J. Mittemeijer: Metall. Mater. Trans. A, 2006, vol. 37A,
30 pp. 319-330.
31
32 [42] B. Ozturk, V.L. Fearing, J.A. Ruth and G. Simkovich: Metall. Trans. A, 1982, vol. 13A,
33 pp. 1871-1873.
34
35 [43] B. Ozturk, V.L. Fearing, J.A. Ruth and G. Simkovich: Solid State Ionics, 1984, vol. 12,
36 pp. 145-151.
37
38 [44] M. Hillert, L. Höglund and J. Ågren: J. Appl. Phys., 2005, vol. 98, 053511 pp. 1-6.
39
40 [45] A. Leineweber: Acta Mat., 2007, vol. 55, pp. 6651-6658.
41
42 [46] J. Philibert: Atom movements, diffusion and mass transport in solids, Les Éditions de
43 Physique (F), 1991.
44
45
46
47
48
49
50
51
52
53
54
55
56
57
58
59
60

Figure Captions

1
2
3
4
5
6
7
8
9
10
11
12
13
14
15
16
17
18
19
20
21
22
23
24
25
26
27
28
29
30
31
32
33
34
35
36
37
38
39
40
41
42
43
44
45
46
47
48
49
50
51
52
53
54
55
56
57
58
59
60

Figure 1: Optical micrograph (cross-sectional view; bright field) of a massive cementite layer (stained) on iron (unstained). The massive cementite layer was generated on ferrite by gaseous nitrocarburising at 823 K for 48 h. The metallographic cross-section was etched with 1 vol.-% Nital containing 1 vol.-% HCl and stained with an alkaline sodium picrate solution (cf. section 2).

Figure 2: Experimentally determined hardness-depth profiles in the ferrite substrate with a massive cementite layer of time-dependent thickness at the surface of the ferrite substrate (dots; cf. hardness axes). Hardness-depth profiles were transformed into nitrogen concentration-depth profiles (dots; cf. nitrogen-concentration axes) applying the calibrated hardness-nitrogen concentration relation (cf. Fig. 3). The simulated nitrogen concentration-depth profiles are shown by the continuous curves. The dashed curves connect the data points pertaining to the hardness/nitrogen concentration-depth profiles for 0.5 h and 2 h, which were not considered for the simulation. Experiments as well as simulations were performed at (a) 783 K, (b) 823 K and (c) 843 K.

Figure 3: Calibration line: Nitrogen concentration (determined by carrier-gas hot extraction; the error is smaller than the size of the dots) vs. the hardness for homogeneous ferrite substrates (determined by micro-Vickers hardness indentations). The straight line was determined by least-squares fitting of Eq. (1) to the experimental data. Solid data points indicate results from nitrided specimens, open data points indicate results from nitrocarburised specimens.

Figure 4: Schematic drawing of a cementite layer on a ferrite substrate (cross-sectional view). A gradient of the chemical potential of nitrogen in cementite provokes the flux of nitrogen

1
2
3 through cementite. Consequently, a nitrogen concentration-depth profile develops in the
4 ferrite substrate, which can be calculated for different time steps and grid points using the
5 model described in section IV and the appendix applying the implicit finite-difference
6 method. Local equilibrium at the gas-solid interface and at the cementite/ferrite interface is
7 assumed.
8
9
10
11
12
13
14
15
16

17 Figure 5: Arrhenius plot: natural logarithm of the product of the partition coefficient and the
18 (tracer-)diffusion coefficient of nitrogen through cementite, $\phi D_{\text{N}}^{*,\text{Fe}_3\text{C}}$, versus the reciprocal
19 temperature $1/T$.
20
21
22
23
24
25
26
27
28
29
30
31
32
33
34
35
36
37
38
39
40
41
42
43
44
45
46
47
48
49
50
51
52
53
54
55
56
57
58
59
60

1
2
3
4
5
6
7
8
9
10
11
12
13
14
15
16
17
18
19
20
21
22
23
24
25
26
27
28
29
30
31
32
33
34
35
36
37
38
39
40
41
42
43
44
45
46
47
48
49
50
51
52
53
54
55
56
57
58
59
60

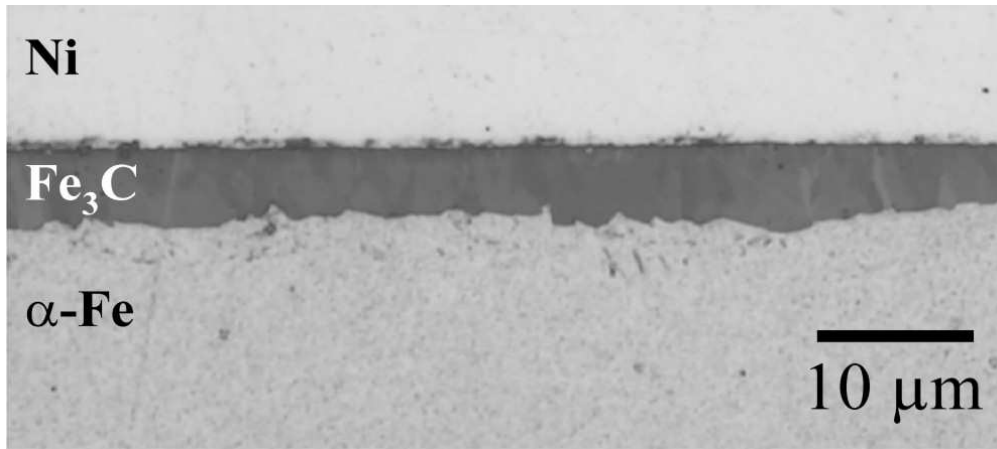


Figure 1
83x37mm (300 x 300 DPI)

Peer Review Only

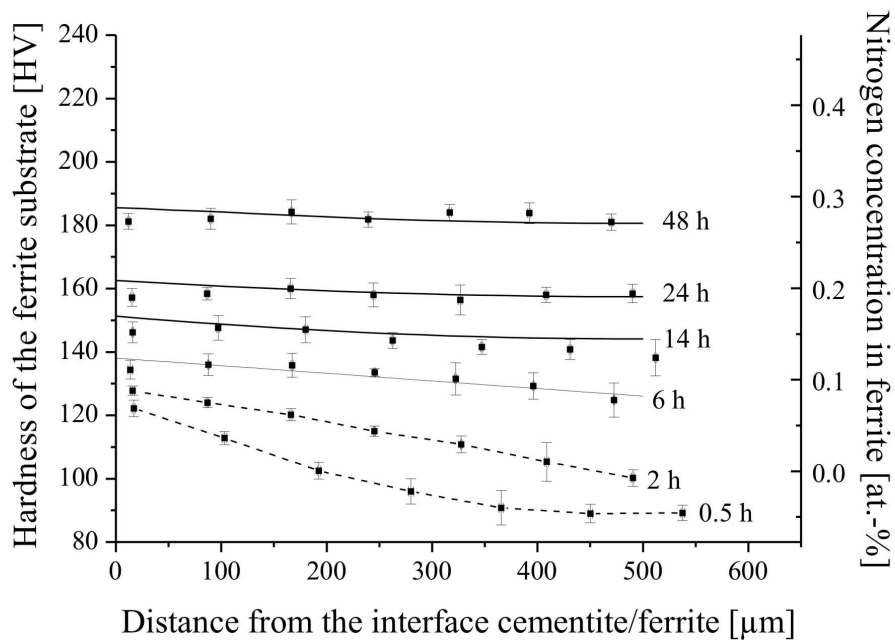


Figure 2a
83x61mm (600 x 600 DPI)

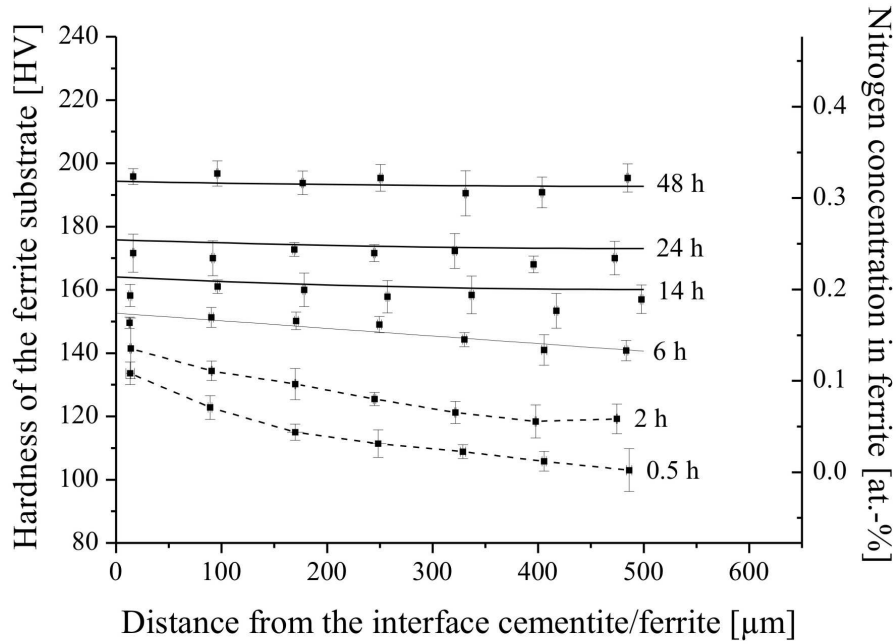


Figure 3b
83x62mm (600 x 600 DPI)

View Only

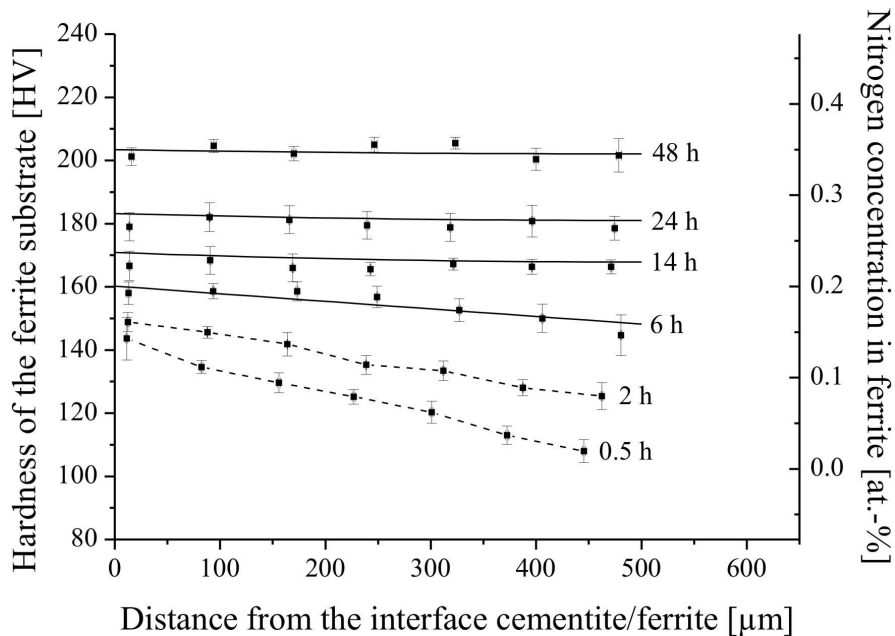


Figure 2c
83x61mm (600 x 600 DPI)

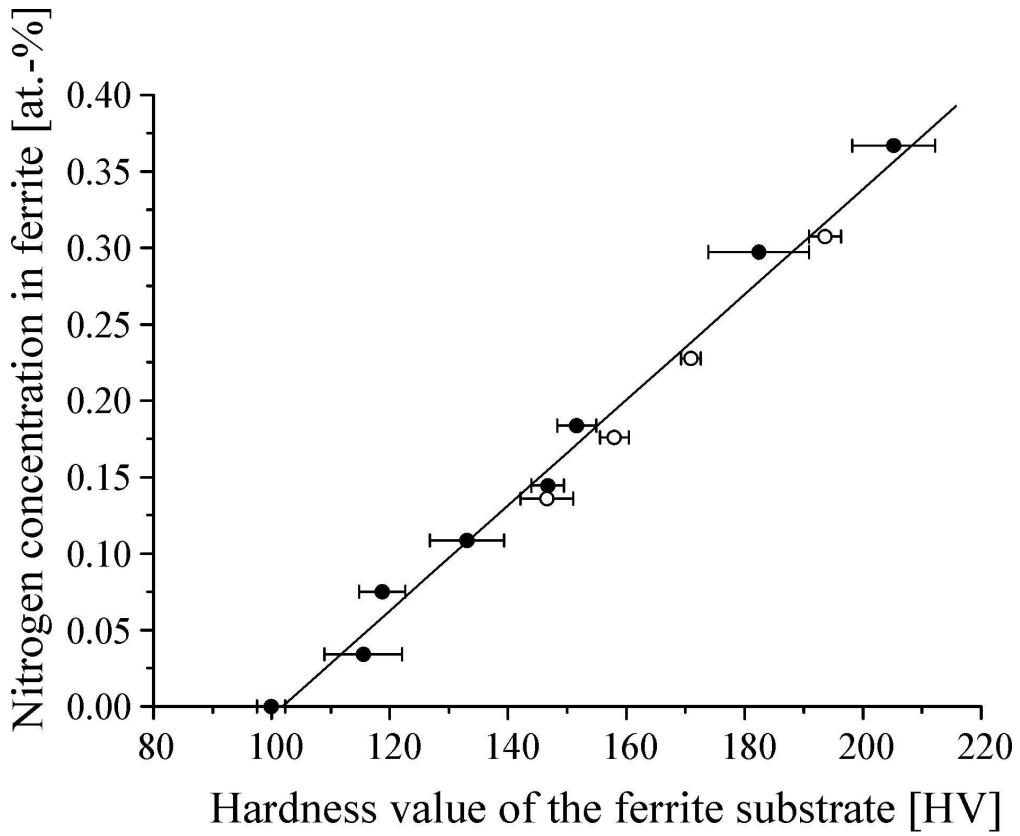


Figure 3
79x65mm (600 x 600 DPI)

Manuscript Only

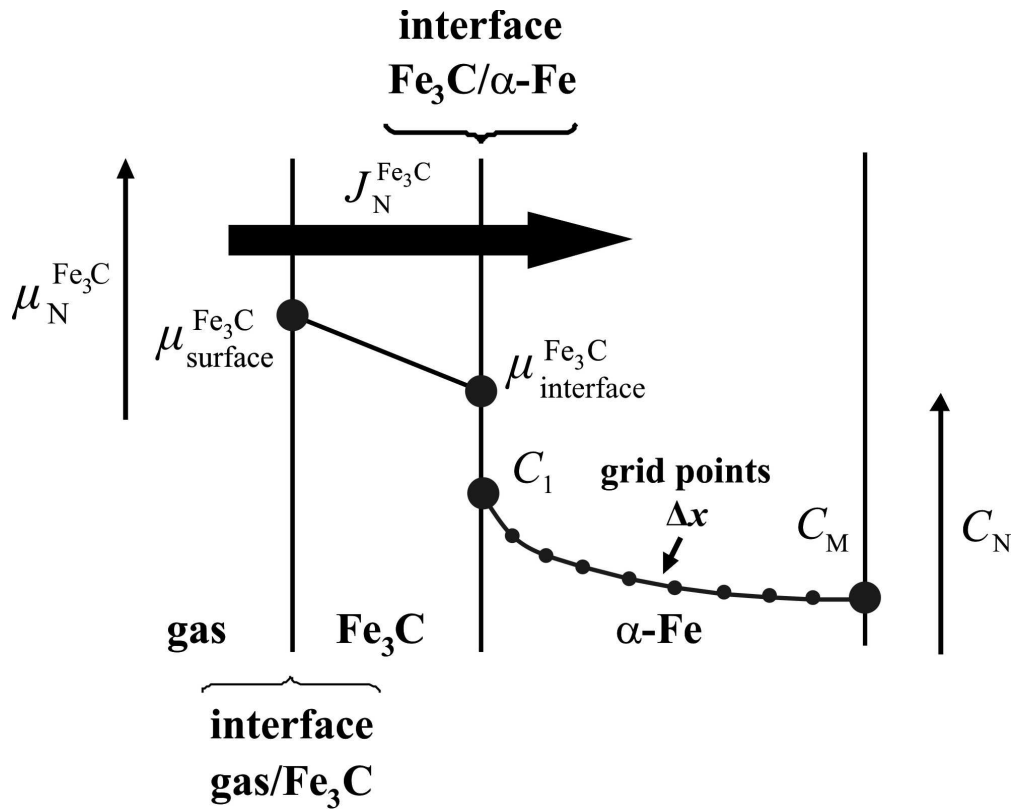


Figure 4
83x67mm (600 x 600 DPI)

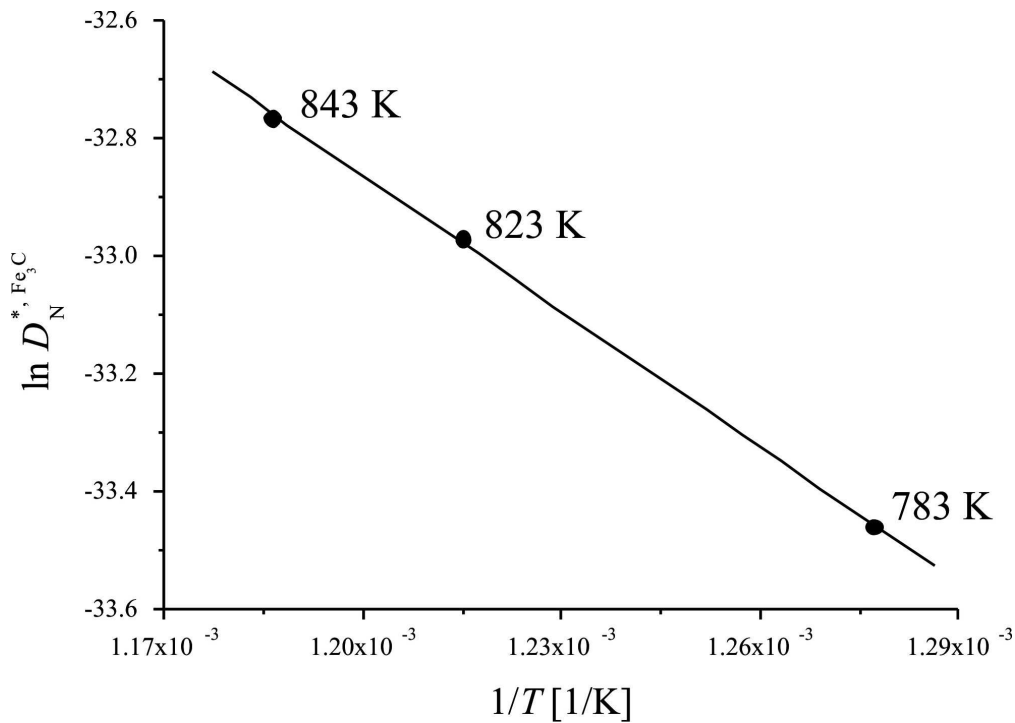


Figure 5
83x59mm (600 x 600 DPI)

ew Only